

Estradiol induces the calcium-dependent translocation of endothelial nitric oxide synthase

REGINA M. GOETZ*[†], HEMANT S. THATTE^{†‡§}, PRAKASH PRABHAKAR*, MICHAEL R. CHO^{‡§}, THOMAS MICHEL*^{¶||}, AND DAVID E. GOLAN^{‡§**}

Divisions of *Cardiology and [‡]Hematology, Department of Medicine, Brigham and Women's Hospital, Boston, MA 02115; [¶]West Roxbury VA Medical Center, West Roxbury, MA 02132; and [§]Department of Biological Chemistry and Molecular Pharmacology, Harvard Medical School, Boston, MA 02115

Communicated by Eva J. Neer, Harvard Medical School, Boston, MA, January 6, 1999 (received for review November 4, 1998)

ABSTRACT Although estrogen is known to stimulate nitric oxide synthesis in vascular endothelium, the molecular mechanisms responsible for this effect remain to be elucidated. Using quantitative immunofluorescence imaging approaches, we have investigated the effect of estradiol on the subcellular targeting of endothelial nitric oxide synthase (eNOS) in bovine aortic endothelial cells. In unstimulated endothelial cells, eNOS is predominantly localized at the cell membrane. Within 5 min after the addition of estradiol, most of the eNOS translocates from the membrane to intracellular sites close to the nucleus. On more prolonged exposure to estradiol, most of the eNOS returns to the membrane. This effect of estradiol is evident at a concentration of 1 pM, and a maximal estradiol effect is seen at a concentration of 1 nM. Neither progesterone nor testosterone has any effect on eNOS distribution. After estradiol addition, a transient rise in intracellular Ca²⁺ concentration precedes eNOS translocation. Both the Ca²⁺-mobilizing and eNOS-translocating effects of estradiol are completely blocked by the estrogen receptor antagonist ICI 182,780, and the intracellular Ca²⁺ chelator 1,2-bis-(*o*-aminophenoxy)ethane-*N,N,N',N'*-tetraacetic acid (BAPTA) prevents estradiol-induced eNOS translocation. Use of the nitric oxide-specific dye diaminofluorescein shows that estradiol treatment increases nitric oxide generation by endothelial cells; this response is blocked by ICI 182,780 and by the eNOS inhibitor *N*^ω-nitro-L-arginine. These results show that estradiol induces subcellular translocation of eNOS by a rapid, Ca²⁺-dependent, receptor-mediated mechanism, and they suggest a nongenomic role for estrogen in the modulation of NO-dependent vascular tone.

Estrogen was identified as a vasodilator nearly 60 years ago. In 1940, Reynolds and Foster reported marked dilation of the ear microvasculature within minutes after injection of estrogen into ovariectomized rabbits (1). The molecular mechanism underlying the estrogen-induced vasodilation is not defined. Several studies suggest that a key mediator of this vasodilator response could be the endothelium-derived relaxing factor, nitric oxide (NO), and that estrogen stimulates NO synthesis in vascular endothelium. Kawano *et al.* (2) found changes in endothelium/NO-dependent vasomotion in parallel with the cyclical hormonal changes in premenopausal women, with the greatest potentiation at peak plasma levels of estrogen. Several groups (3–5) reported that estrogen potentiates or restores endothelium-dependent coronary vasodilation in postmenopausal women; Guetta *et al.* (6) showed that these effects are mediated by NO. Van Buren *et al.* (7) and Rosenfeld *et al.* (8) identified NO as the principal mediator of estrogen-induced dilation of ovine uterine vasculature. More recently, Lantin-Hermoso *et al.* (9) and Caulin-Glaser *et al.* (10) found that

estrogen activates the endothelial isoform of NO synthase (eNOS) in cultured endothelial cells. Together, these studies suggest that estrogen acts as a vasodilator by stimulation of endothelial NO synthesis, although the molecular mechanism underlying this effect remains to be elucidated.

eNOS is a Ca²⁺/calmodulin-dependent enzyme and is subject to a complex pattern of intracellular regulation, including co- and post-translational modifications and diverse interactions with other proteins and ligands (reviewed in refs. 11 and 12). In endothelial cells and cardiac myocytes eNOS is localized in specialized plasmalemmal signal-transducing domains termed caveolae; acylation of the enzyme by the fatty acids myristate and palmitate is required for targeting of the protein to caveolae. Other proteins that participate in the regulation of eNOS are also sequestered in these plasmalemmal domains, including the G protein-coupled bradykinin B₂ and muscarinic cholinergic m₂ receptors (13, 14). Targeting of eNOS to caveolae may thus facilitate its coupling to and activation by these signaling molecules.

In unstimulated endothelial cells, the eNOS enzyme is tonically inhibited by its protein-protein interactions with caveolin, the resident scaffolding protein in caveolae. Cell stimulation with Ca²⁺-mobilizing agonists such as bradykinin promotes calmodulin binding to eNOS and caveolin dissociation from the enzyme, rendering the enzyme active; as intracellular Ca²⁺ returns to basal levels, calmodulin dissociates from the enzyme and the inhibitory eNOS-caveolin complex reforms (15). On more prolonged cell stimulation with bradykinin, eNOS is redistributed from particulate to more soluble cellular fractions, concomitant with depalmitoylation and increased phosphorylation of the enzyme (16). Our recent imaging studies have provided additional information on eNOS cellular targeting, revealing that Ca²⁺-mobilizing agonists such as bradykinin induce translocation of eNOS from the plasmalemma to intracellular sites close to the nucleus (17). Using these recently established quantitative cell imaging approaches (17), we here explore the effect of estradiol on eNOS cellular targeting. Our studies show that estradiol induces translocation of eNOS by a Ca²⁺-dependent, receptor-mediated mechanism.

Abbreviations: BAEC, bovine aortic endothelial cells; BAPTA/AM, 1,2-bis-(*o*-aminophenoxy)ethane-*N,N,N',N'*-tetraacetic acid tetra(acetoxymethyl) ester; DAF-2/DA, 4,5-diaminofluorescein diacetate; eNOS, endothelial nitric oxide synthase; ICI 182,780, 7 α -[9-[(4,4,5,5,5-pentafluoropentyl)sulfonyl]nonyl]estra-1,3,5(10)-triene-3,17 β -diol; NNA, *N*^ω-nitro-L-arginine.

[†]R.M.G. and H.S.T. contributed equally to this work.

^{||}To whom reprint requests may be addressed at: Cardiovascular Division, Brigham and Women's Hospital, Thorn Building, Room 1210A, 75 Francis Street, Boston, MA 02115. e-mail: michel@calvin.bwh.harvard.edu.

^{**}To whom reprint requests may be addressed at: Department of Biological Chemistry and Molecular Pharmacology, Harvard Medical School, Seeley G. Mudd Building, Room 304, 250 Longwood Avenue, Boston, MA 02115. e-mail: dgolan@hms.harvard.edu.

The publication costs of this article were defrayed in part by page charge payment. This article must therefore be hereby marked "advertisement" in accordance with 18 U.S.C. §1734 solely to indicate this fact.

PNAS is available online at www.pnas.org.

MATERIALS AND METHODS

Reagents. Cell culture media and penicillin–streptomycin were from Life Technologies (Rockville, MD). Fetal bovine serum was from HyClone (Logan, UT). Anti-eNOS monoclonal antibody was from Transduction Laboratories (Lexington, KY). Rhodamine-conjugated goat anti-mouse antibody was from Pierce (Rockford, IL). Fluo-3/AM was from Molecular Probes (Eugene, OR). 1,2-Bis-(*o*-aminophenoxy)ethane-*N,N,N',N'*-tetraacetic acid tetra(acetoxymethyl) ester (BAPTA/AM) and 4,5-diaminofluorescein diacetate (DAF-2/DA) were from Calbiochem–Novabiochem (San Diego, CA). 7α -[9-[(4,4,5,5-Pentafluoropentyl)sulfinyl]nonyl]estra-1,3,5(10)-triene-3,17 β -diol (ICI 182,780) was from Tocris Cookson (Ballwin, MO). Estradiol, progesterone, testosterone (each as the water-soluble cyclodextrin complex), and all other reagents were from Sigma (St. Louis, MO).

Cell Culture and Drug Treatments. Bovine aortic endothelial cells (BAEC) were from Cell Systems (Kirkland, WA) and were maintained in culture in Dulbecco's modified Eagle's medium (DMEM) supplemented with 10% heat-inactivated fetal bovine serum, 200 units/ml penicillin, and 200 μ g/ml streptomycin (18). Cells were studied at passage 6 and at 40% confluency. Drug treatments were performed in phenol red-free DMEM supplemented with fetal bovine serum and antibiotics. Stock solutions of ICI 182,780, BAPTA/AM, and DAF-2/DA were prepared in dimethyl sulfoxide and were used at 1:2000 (ICI 182,780, BAPTA/AM) or 1:500 (DAF-2/DA) dilution. All other drugs were dissolved in phenol red-free DMEM. For studying effects of BAPTA, cells were incubated with 20 μ M BAPTA/AM 20 min before stimulation.

Immunolabeling. BAEC were cultured onto gelatin-coated glass coverslips on the day before microscopic analysis. After drug treatment at 37°C in a humidified atmosphere with 5% CO₂, cells were fixed in 2% freshly prepared paraformaldehyde for 10 min at room temperature and permeabilized in phosphate-buffered saline (PBS; Dulbecco's formulation) with 0.1% Triton X-100 and 0.1% bovine serum albumin for 5 min at room temperature. Cells were then incubated in PBS containing 10% goat serum overnight at 4°C, treated with anti-eNOS monoclonal antibody at 1:250 dilution for 60 min at room temperature, washed with PBS three times for 5 min each, and incubated with rhodamine-conjugated goat anti-mouse antibody at 1:200 dilution for 60 min at room temperature. After washing with PBS three times for 10 min each, the coverslip bearing the cells was mounted on a microscope slide and sealed with nail polish.

Microscopy and Quantitative Analysis of eNOS Immunofluorescence. Cell imaging and quantitative analysis were performed as previously described (17). A Zeiss epifluorescence microscope was used to observe cells at $\times 250$ to $\times 1000$ magnification. A conservative criterion was chosen for quantifying the presence of eNOS immunofluorescence at the plasma membrane. Since the eNOS immunofluorescence at the membrane was usually nonuniform in each individual cell, a cell was assigned as eNOS membrane-positive if even a small patch of membrane-associated eNOS was detected. These analyses were performed in a completely blinded fashion. For each experiment, at least 100 cells per coverslip were analyzed, and the proportion of eNOS membrane-positive cells was normalized to that found under basal conditions. The data are presented as the average of at least three blinded experiments performed on different days; both intra- and interexperimental variability were less than 5%.

Determination of Intracellular Calcium Ion Concentration. The concentration of intracellular calcium ions was determined by using the calcium indicator dye Fluo-3, as previously described (17). Cells were incubated with 10 μ M Fluo-3/AM in Hanks' balanced salt solution (HBSS) for 60 min at room

temperature. After washing with HBSS, the coverslip bearing the cells was mounted on a custom-made microscopy chamber that allowed rapid exchange of medium without disturbing the cells. Cells were stimulated with 100 nM estradiol in the presence or absence of 10 μ M ICI 182,780, by rapidly removing the mounting medium and adding fresh medium containing drug(s). Cells were studied by epifluorescence microscopy using a cooled charge-coupled device camera, and Fluo-3 fluorescence counts were recorded in real time before and after drug treatment. Typically, 6–12 cells were identified in a field of view at $\times 25$ magnification, and changes in the integrated fluorescence intensity of each cell were monitored over time. Cell boundaries were drawn by using an image processor (MetaMorph; Universal Imaging, West Chester, PA), and fluorescence intensity was integrated over all pixels within the boundary of each individual cell. Because the size and shape of the cells were variable, and to eliminate effects because of variation in Fluo-3 dye loading, the fluorescence intensities from each image were normalized by those from a reference image recorded before drug treatments. Background intensity was subtracted from each image.

Determination of Intracellular NO Generation. The generation of intracellular NO was determined by using the NO indicator dye DAF-2, as recently described (19, 20). In this method, cells are loaded with the membrane-permeant diacetate form of DAF-2, which is cleaved by cellular esterases to a membrane-impermeant form. This dye is then capable of combining with intracellularly generated NO to yield the brightly fluorescent triazolofluorescein derivative (19, 20). Cells were incubated with 10 μ M DAF-2/DA in DMEM for 60 min at 37°C. After washing with DMEM, the coverslip bearing the cells was mounted as described above. Cells were stimulated with 100 nM estradiol in the presence or absence of 100 μ M *N*^ω-nitro-L-arginine (NNA) or of 10 μ M ICI 182,780, as described above. Cells were studied by epifluorescence microscopy as described above; DAF-2 fluorescence counts were recorded in real time before and 15 min after drug treatment.

RESULTS AND DISCUSSION

The patterns of eNOS immunofluorescence in BAEC under basal conditions and after treatment with estradiol (100 nM, 15 min) are shown in Fig. 1. Specificity of eNOS labeling was demonstrated by performing cell labeling with nonimmune IgG1 instead of anti-eNOS monoclonal antibody; under these conditions, no significant cellular fluorescence was detected (data not shown). As previously observed (17), under basal conditions the pattern of eNOS immunofluorescence was heterogeneous within and between BAEC. Typically, 60–80% of cells showed prominent eNOS immunostaining at the plasma membrane, while the remaining 20–40% of cells showed only a patchy intracellular (predominantly perinuclear) pattern of eNOS immunofluorescence (Fig. 1A). Although the proportion of cells with eNOS immunostaining at the membrane ranged from 50% to more than 90%, this value was consistent under identical experimental conditions within duplicate analyses. Such heterogeneity may reflect the multiple cellular processes that affect eNOS targeting and were not definitively controlled in these experiments. Even within a single cell with membrane-associated eNOS, the fluorescence at the membrane was typically nonuniform, with eNOS-positive patches of various sizes juxtaposed with eNOS-negative regions (Fig. 1). Heterogeneous staining at the membrane has also been observed for other proteins (17, 21–25), and we and others have found patchy intracellular staining for other proteins targeted to caveolae (i.e., caveolin, the cationic amino acid transporter-1, c-Src tyrosine kinase, and the high density lipoprotein receptor SR-BI) and for noncaveolar membrane proteins (i.e., the Na⁺/K⁺-ATPase and the cholestero-

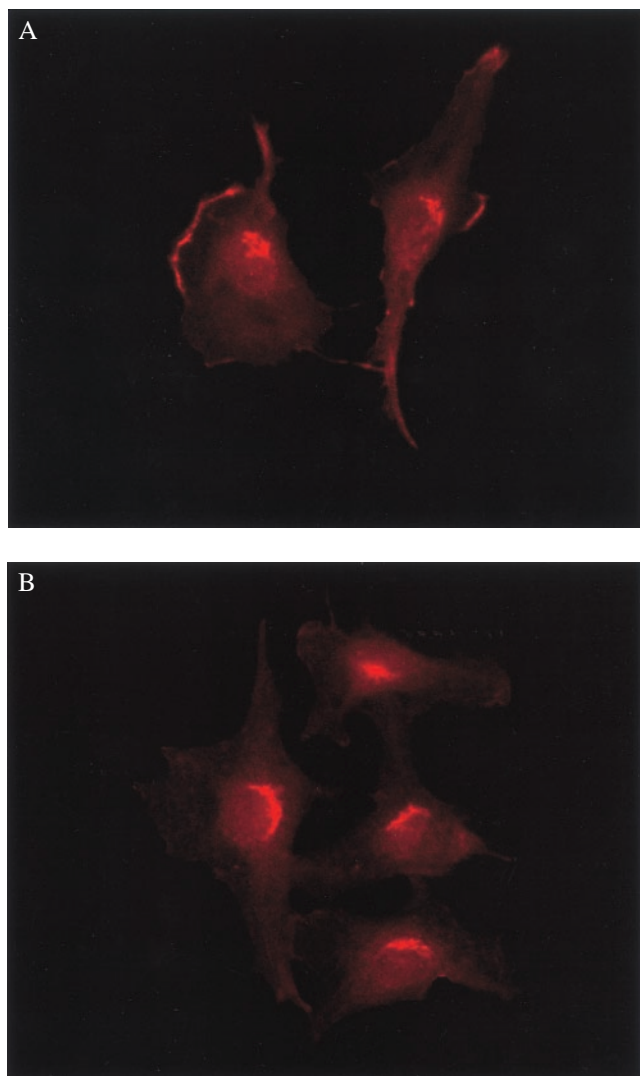


FIG. 1. Translocation of eNOS in endothelial cells in response to estradiol. Shown are typical photomicrographs of bovine aortic endothelial cells processed for eNOS immunofluorescence as described in the text. (A) Representative image of cells analyzed under basal conditions. (B) Representative image of cells treated with 100 nM 17β -estradiol for 15 min before immunolabeling for eNOS protein. Both images are at $\times 25$ magnification and printed with identical brightness and contrast settings.

kinin receptor) (17, 21–25). After treatment with estradiol the pattern of eNOS immunofluorescence in BAEC changed profoundly. Estradiol induced a dramatic redistribution of eNOS from the plasma membrane to an intracellular site close to the nucleus (Fig. 1B).

Quantitative immunofluorescence microscopy was used to characterize further the effect of estradiol (17). Given the intra- and intercellular heterogeneity of eNOS immunofluorescence, a cell with any detectable fluorescence at the plasma membrane was assigned as “eNOS membrane-positive,” whereas a cell with no such fluorescence was assigned as “eNOS membrane-negative.” Because the proportion of cells scored as eNOS membrane-positive under basal conditions was variable from experiment to experiment, for each experiment the data were normalized to the respective basal value. The first series of experiments sought to determine the pharmacological specificity of the estradiol effect (Fig. 2). BAEC were treated for 15 min with estradiol, progesterone, or testosterone (100 nM each), then immunolabeled and analyzed for membrane-associated eNOS. Estradiol induced a 50% loss

of membrane-associated eNOS, whereas neither progesterone nor testosterone had any effect on the cellular distribution of the enzyme. Estradiol-induced translocation of eNOS was completely blocked by the estrogen receptor antagonist ICI 182,780 (10 μ M), whereas ICI 182,780 alone had no effect on eNOS distribution. These results indicate that estradiol-induced translocation of eNOS is hormone-specific and receptor-mediated. Even under experimental conditions showing a maximal response to estradiol, a significant fraction of the cells (20–50%) failed to show any eNOS translocation in response to drug treatment. The explanation for this cellular heterogeneity is not clear, although differential expression of eNOS and other proteins by endothelial cells has also been documented in the intact vascular wall (26, 27). The heterogeneity in eNOS staining and estradiol responsiveness seen in our experimental system may thus simply reflect this intrinsic regional diversity of endothelial cell gene expression, and it suggests that some of the factors that lead to differences in endothelial cell phenotype are recapitulated in our cell culture model (28).

We next performed dose–response and time-course analyses of eNOS translocation by estradiol. For the dose–response analysis, BAEC were treated for 15 min with different concentrations of estradiol, then immunolabeled and analyzed for membrane-associated eNOS (Fig. 3). The EC_{50} for eNOS translocation by estradiol was 400 pM, and the maximum effect was seen at a concentration of 1 nM. These concentrations are similar to those found in the plasma of normal premenopausal women (29). Compared with the dose–response for eNOS translocation by bradykinin (17), estradiol was nearly equally effective at lower concentrations but less effective at higher concentrations.

For the time-course analysis BAEC were treated with 1 μ M estradiol for different times, then processed and analyzed for membrane-associated eNOS (Fig. 4). Within 5 min of treatment the maximum effect of estradiol was seen, with about 60% of cells devoid of membrane-associated eNOS. On more prolonged estradiol treatment the proportion of membrane-associated eNOS gradually recovered, reaching nearly basal values after 60 min. To exclude potential effects on eNOS distribution caused by changes in eNOS protein expression with prolonged estradiol treatment, in a separate experiment the total amount of cellular eNOS protein was determined at each time point. There was no change in the amount of eNOS protein from 0 to 90 min of estradiol treatment (data not shown).

The temporal pattern of eNOS translocation by estradiol resembles that of eNOS translocation in response to bradykinin (17), suggesting that these two events could be mediated by similar signaling pathways. Because bradykinin-induced eNOS translocation is strictly Ca^{2+} -dependent (17), we explored the role of Ca^{2+} in eNOS translocation in response to estradiol. First, the effect of estradiol on intracellular $[Ca^{2+}]$ was studied in BAEC. Cells were loaded with the Ca^{2+} indicator dye Fluo-3, then stimulated with 100 nM estradiol while the fluorescence emission of intracellular Fluo-3 was measured simultaneously. As shown in Fig. 5, estradiol induced a rapid rise in intracellular $[Ca^{2+}]$. The peak level was reached within 30 sec of incubation with the hormone, then intracellular $[Ca^{2+}]$ decreased within 1 min and returned to baseline within 15 min of hormone treatment. Although these changes in intracellular Ca^{2+} were different from those induced by bradykinin in these cells (17), others have observed a similar Ca^{2+} response to estradiol in other cell types (30, 31). The estrogen receptor antagonist ICI 182,780 (10 μ M) completely blocked the estradiol-induced rise in intracellular $[Ca^{2+}]$, showing that this effect of estradiol is receptor-mediated. Further, the temporal patterns of estradiol-induced intracellular Ca^{2+} changes and eNOS translocation suggest that the Ca^{2+} spike precedes eNOS translocation.

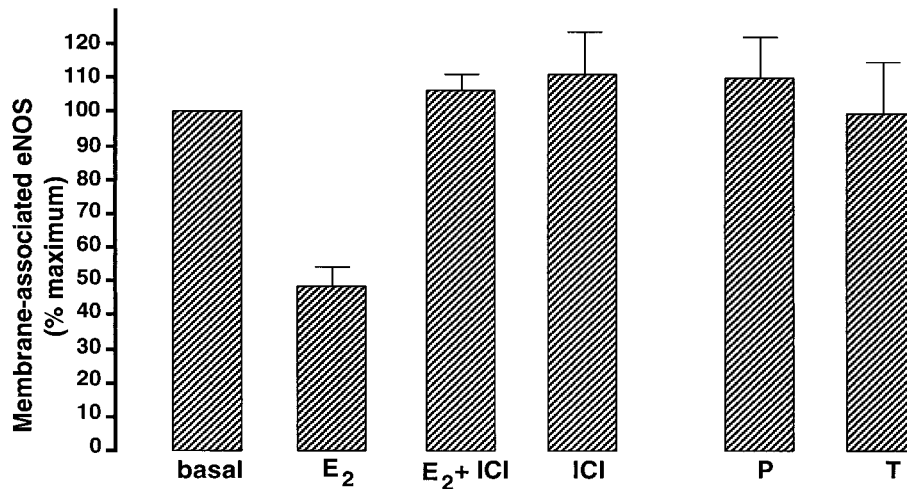


FIG. 2. Specificity of eNOS translocation in response to estradiol. BAEC were incubated for 15 min with 17β -estradiol (E₂, 100 nM), the estrogen receptor antagonist ICI 182,780 (ICI, 10 μ M), 17β -estradiol plus ICI 182,780 (E₂, 100 nM + ICI, 10 μ M), progesterone (P, 100 nM), or testosterone (T, 100 nM) and then processed for eNOS immunofluorescence as described in the text. The percentage of untreated (basal) cells with eNOS immunoreactivity at the plasma membrane was determined and used to normalize the percentage of cells with membrane-positive eNOS immunoreactivity observed for each drug treatment. That is, for each individual experiment the basal level of eNOS immunoreactivity at the plasma membrane was set equal to 100%. At least 100 cells were analyzed for each treatment. Each data point represents the mean \pm standard error of the mean of at least three separate experiments.

We next studied the effect of intracellular Ca²⁺ chelation on estradiol-induced eNOS translocation. BAEC were loaded with the Ca²⁺ chelator BAPTA, then stimulated with 100 nM estradiol for 15 min and processed for analysis of eNOS membrane targeting. As shown in Fig. 6, intracellular Ca²⁺ chelation completely blocked the effect of estradiol on the cellular distribution of eNOS. These results show that the estradiol-induced translocation of eNOS is strictly dependent on intracellular Ca²⁺, a result that is consistent with our previous findings on eNOS translocation in response to bradykinin (17). Lantin-Hermoso *et al.* (9) have also found that eNOS activation by estradiol is Ca²⁺ dependent, although Caulin-Glaser *et al.* (10) have suggested that estradiol may

activate eNOS independently of cytosolic Ca²⁺ mobilization. Different cell culture and experimental conditions may explain these apparently incompatible observations.

Our final series of experiments was designed to confirm that treatment of BAEC with estradiol induced functional activation of eNOS. BAEC were loaded with the newly described NO-sensitive dye DAF-2, then stimulated with 100 nM estradiol for 15 min. DAF-2 fluorescence was recorded before and after estradiol treatment. As shown in Fig. 7, estradiol stimulated a significant increase in intracellular NO generation; this effect was inhibited completely by treatment with the eNOS inhibitor NNA or with the estrogen receptor antagonist

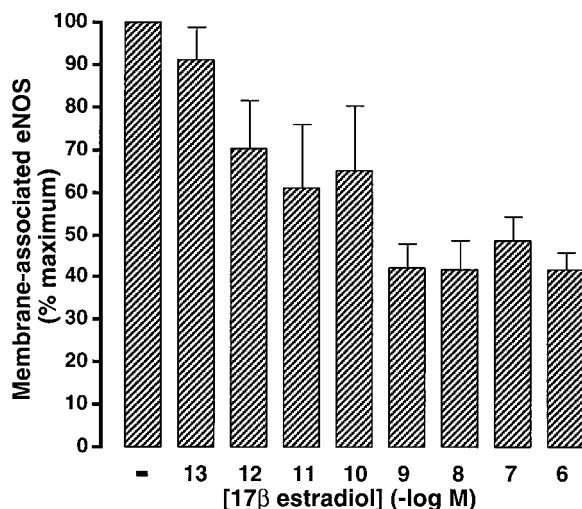


FIG. 3. Translocation of eNOS in endothelial cells: estradiol dose-response. Bovine aortic endothelial cells were incubated for 15 min with different concentrations of 17β -estradiol as shown, and then processed for eNOS immunofluorescence as described in the text. The percentage of untreated cells with eNOS immunoreactivity at the plasma membrane was determined and was used to normalize the percentage of cells with membrane-positive eNOS immunoreactivity observed at each dose of estradiol. For each treatment, at least 100 cells were analyzed. Each data point represents the mean \pm standard error of the mean of at least three separate experiments.

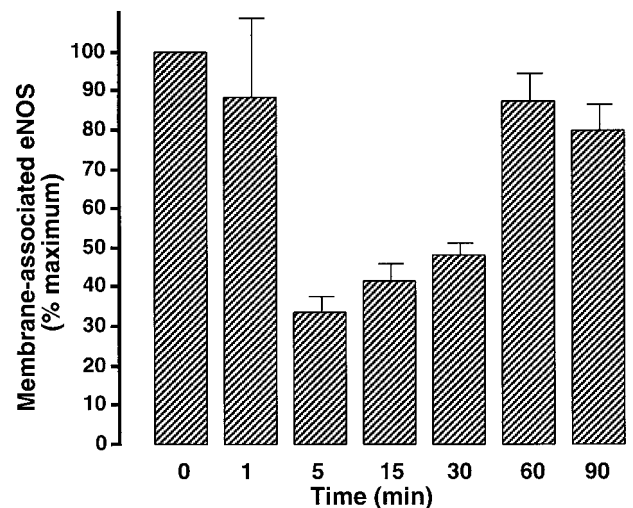


FIG. 4. Time course of eNOS translocation in response to estradiol. Bovine aortic endothelial cells were incubated with 1 μ M 17β -estradiol for different times as shown and then processed for eNOS immunofluorescence as described in the text. The percentage of untreated cells with eNOS immunoreactivity at the plasma membrane was determined at time point zero and at each of the subsequent time points; these fractions were used to normalize the percentage of cells with membrane-positive eNOS immunoreactivity at each time after drug treatment. For each time point, at least 100 cells were analyzed. Each data point represents the mean \pm standard error of the mean of at least three separate experiments.

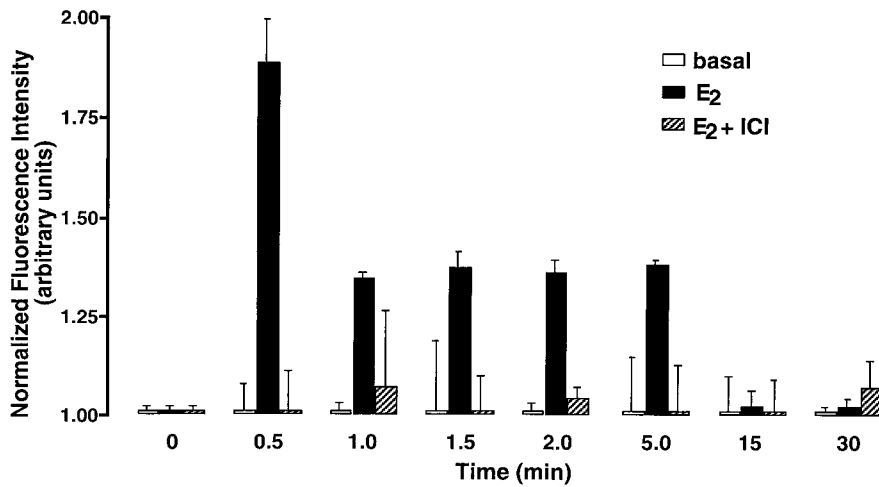


FIG. 5. Effects of estradiol on intracellular calcium in endothelial cells. BAEC were incubated with the calcium indicator dye Fluo-3/AM and processed for intracellular calcium ion concentration measurements, as described in the text. The integrated Fluo-3 fluorescence intensity of each cell (arbitrary units) was measured in real time after treatment with either estradiol (E₂, 100 nM) or estradiol plus ICI 182,780 (E₂, 100 nM + ICI, 10 μM) and was normalized by the fluorescence intensity for that cell before treatment. For each time point, 22 cells were analyzed in three separate experiments. Each data point represents the mean ± standard error of the mean.

ICI 182,780. These data show that, under the conditions used here, intracellular NO generation requires both estradiol-mediated stimulation of the estrogen receptor and functional activation of eNOS.

Classically, estrogen and other steroid hormones are thought to bind to an intracellular receptor which, upon ligand binding, acts as a transcription regulatory factor. However, the characteristics of eNOS translocation in response to estradiol, in particular its rapidity and reversibility, are incompatible with a genomic mechanism of estrogen action. Rather, the present effect of estradiol is better explained by a mechanism of action involving cell surface receptors. The first evidence for specific binding sites for estrogen at the cell membrane was provided by Pietras and Szego more than 20 years ago (32). Since then, the concept of a nongenomic mechanism of steroid action has emerged from numerous studies on the rapid effects of steroid hormones (reviewed in ref. 33). For the present study, as for these other reports of rapidly mediated cellular responses to

estrogen, the identity and regulation of the receptor(s) that modulates nongenomic effects of estrogen remain unknown. Here we show that the estradiol-induced translocation of eNOS is strictly Ca²⁺-dependent and temporally associated with the estrogen-induced rise and fall in intracellular Ca²⁺ concentration. Beyond this observation, the molecular mechanisms underlying eNOS translocation in response to estradiol are less well understood.

The role of eNOS translocation in the regulation of NO formation and release by estradiol remains a matter of speculation. The time course of eNOS activation is much more rapid than the time course of enzyme translocation in the endothelial cell. It is plausible that translocation of eNOS from the cell membrane to intracellular sites could provide a means to uncouple the enzyme from its activators, and thereby

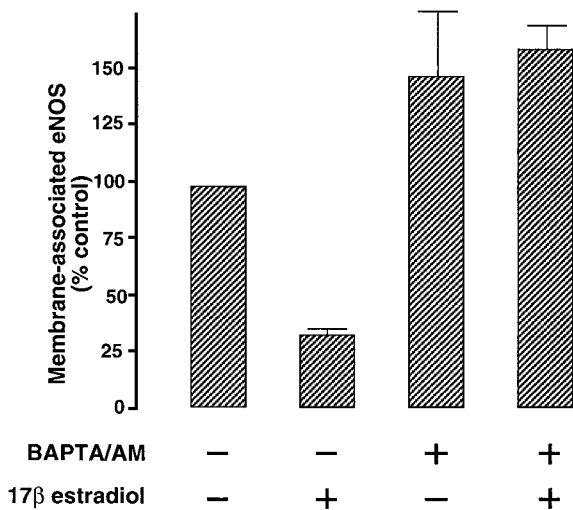


FIG. 6. Effects of intracellular calcium chelation on estradiol-induced eNOS translocation. BAEC were treated with 20 μM BAPTA/AM for 20 min, stimulated with 100 nM estradiol for 15 min, then processed and analyzed for eNOS immunostaining as described in the text. Each data point represents the mean ± standard error of the mean of three separate experiments.

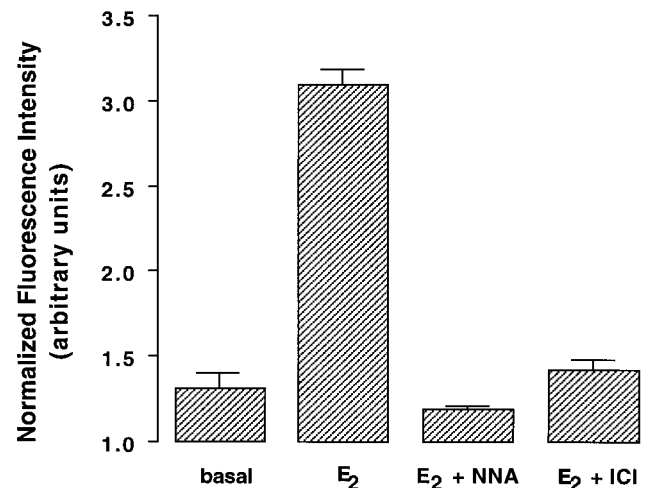


FIG. 7. Effects of estradiol on nitric oxide generation in endothelial cells. Bovine aortic endothelial cells were incubated with the NO indicator dye DAF-2/DA and processed for intracellular NO generation measurements, as described in the text. The integrated DAF-2 fluorescence intensity of each cell (arbitrary units) was measured after 15 min of treatment with estradiol (E₂, 100 nM), estradiol plus NNA (E₂, 100 nM + NNA, 100 μM), or estradiol plus ICI 182,780 (E₂, 100 nM + ICI, 10 μM), and normalized by the fluorescence intensity for that cell before treatment. For each treatment, 30 cells were analyzed in three separate experiments. Each data point represents the mean ± standard error of the mean.

attenuate the formation and release of NO. Alternatively, translocation of the enzyme could play a role in redirecting the formation and release of NO to specific, as yet unidentified, intracellular sites. The present study has established a role for estradiol in the Ca²⁺-dependent regulation of eNOS targeting, thereby identifying another potential point for modulation of NO signal transduction in the vascular endothelium.

This work was supported by awards from the National Institutes of Health (to T.M. and D.E.G.) and from the American Heart Association and the Burroughs Wellcome Fund (to T.M.). T.M. is a Burroughs Wellcome Scholar in Experimental Therapeutics. R.M.G. is the recipient of a postdoctoral research fellowship from the Deutsche Forschungsgemeinschaft. H.S.T. is supported by a National Research Service Senior Fellowship Award (National Institutes of Health). P.P. is supported by a fellowship from the Brigham and Women's Hospital Research Organization. M.R.C. is supported by a grant from the Whitaker Foundation.

1. Reynolds, S. R. M. & Foster, F. I. (1940) *J. Pharmacol. Exp. Ther.* **68**, 173–178.
2. Kawano, H., Motoyama, T., Kugiyama, K., Hirashima, O., Ohgushi, M., Yoshimura, M., Ogawa, H., Okumura, K. & Yasue, H. (1996) *Proc. Assoc. Am. Physicians* **108**, 473–480.
3. Reis, S. E., Gloth, S. T., Blumenthal, R. S., Resar, J. R., Zacur, H. A., Gerstenblith, G. & Brinker, J. A. (1994) *Circulation* **89**, 52–60.
4. Gilligan, D. M., Quyyumi, A. A. & Cannon, R. O. (1994) *Circulation* **89**, 2545–2551.
5. Collins, P., Rosano, G. M. C., Sarrel, P. M., Ulrich, L., Adamopoulos, S., Beale, C. M., McNeill, J. G. & Poole-Wilson, P. A. (1995) *Circulation* **92**, 24–30.
6. Guetta, V., Quyyumi, A. A., Prasad, A., Panza, J. A., Waclawiw, M. & Cannon, R. O. (1997) *Circulation* **96**, 2795–2801.
7. Van Buren, G. A., Yang, D. & Clark, K. E. (1992) *Am. J. Obstet. Gynecol.* **167**, 828–833.
8. Rosenfeld, C. R., Cox, B. E., Roy, T. & Magness, R. R. (1996) *J. Clin. Invest.* **98**, 2158–2166.
9. Lantin-Hermoso, R. L., Rosenfeld, C. R., Yuhanna, I. S., German, Z., Chen, Z. & Shaul, P. W. (1997) *Am. J. Physiol.* **273**, 119–126.
10. Caulin-Glaser, T., Garcia-Cardena, G., Sarrel, P., Sessa, W. C. & Bender, J. R. (1997) *Circ. Res.* **81**, 885–892.
11. Sase, K. & Michel, T. (1997) *Trends Cardiovasc. Med.* **7**, 25–34.
12. Michel, T. & Feron, O. (1997) *J. Clin. Invest.* **100**, 2146–2152.
13. de Weerd, W. F. C. & Leeb-Lundberg, L. M. F. (1997) *J. Biol. Chem.* **272**, 17858–17866.
14. Feron, O., Smith, T. W., Michel, T. & Kelly, R. A. (1997) *J. Biol. Chem.* **272**, 17744–17748.
15. Feron, O., Saldana, F., Michel, J. B. & Michel, T. (1998) *J. Biol. Chem.* **273**, 3125–3128.
16. Robinson, L. J., Busconi, L. & Michel, T. (1995) *J. Biol. Chem.* **270**, 995–998.
17. Prabhakar, P., Thatte, H. S., Goetz, R. M., Cho, M. R., Golan, D. E. & Michel, T. (1998) *J. Biol. Chem.* **273**, 27383–27388.
18. Lamas, S., Marsden, P. M., Li, G. K., Tempst, P. & Michel, T. (1992) *Proc. Natl. Acad. Sci. USA* **89**, 6348–6352.
19. Kojima, H., Sakurai, K., Kikuchi, K., Kawahara, S., Kirino, Y., Nagoshi, H., Hirata, Y. & Nagano, T. (1998) *Chem. Pharm. Bull.* **46**, 373–375.
20. Nakatsubo, N., Kojima, H., Kikuchi, K., Nagoshi, H., Hirata, Y., Maeda, D., Imai, Y., Irimura, T. & Nagano, T. (1998) *FEBS Lett.* **427**, 263–266.
21. Smart, E. J., Ying, Y., Conrad, P. A. & Anderson, R. G. W. (1994) *J. Cell Biol.* **127**, 1185–1197.
22. McDonald, K. K., Zharikov, S., Block, E. R. & Kilberg, M. S. (1997) *J. Biol. Chem.* **272**, 31213–31216.
23. Li, S., Couet, J. & Lisanti, M. P. (1996) *J. Biol. Chem.* **271**, 29182–29190.
24. Babitt, J., Trigatti, B., Rigotti, A., Smart, E. J., Anderson, R. G. W., Xu, S. & Krieger, M. (1997) *J. Biol. Chem.* **272**, 13242–13249.
25. Roettger, B. F., Rentsch, R. U., Pinon, D., Holicky, E., Hadac, E., Larkin, J. M. & Miller, L. J. (1995) *J. Cell Biol.* **128**, 1029–1041.
26. Andries, L. J., Brutsaert, D. L. & Sys, S. U. (1998) *Circ. Res.* **82**, 195–203.
27. Gabriels, J. E. & Paul, D. L. (1998) *Circ. Res.* **83**, 636–643.
28. Aird, W. C., Jahroudi, N., Weiler-Guettler, H., Rayburn, H. B. & Rosenberg, R. D. (1995) *Proc. Natl. Acad. Sci. USA* **92**, 4567–4571.
29. Abraham, G. E., Odell, W. D., Swerdloff, R. S. & Hopper, K. (1972) *J. Clin. Endocrinol. Metab.* **34**, 312–318.
30. Morley, P., Whitfield, J. F., Vanderhyden, B. C., Tsang, B. K. & Schwartz, J. (1992) *Endocrinology* **131**, 1305–1312.
31. Le Malley, V., Grosse, B. & Lieberherr, M. (1997) *J. Biol. Chem.* **272**, 11902–11907.
32. Pietras, R. J. & Szego, C. M. (1977) *Nature (London)* **265**, 69–72.
33. Wehling, M. (1997) *Annu. Rev. Physiol.* **59**, 365–393.